

A SUBFAMILY OF DR ADHESINS OF *Escherichia coli* BIND INDEPENDENTLY TO DECAY-ACCELERATING FACTOR AND THE N-DOMAIN OF CARCINOEMBRYONIC ANTIGEN*

Natalia Korotkova¹, Ernesto Cota², Yuri Lebedin³, Severine Monpouet², Julie Guignot⁴, Alain L. Servin⁴, Steve Matthews² and Steve Moseley¹

From: ¹Department of Microbiology, University of Washington, Seattle, WA 98195-7242; ²Division of Molecular Biosciences, Imperial College London, South Kensington, London, SW7 2AZ, UK; ³Xema-Medica Co., Moscow, Russia; and ⁴Institut National de la Santé et de la Recherche Medicalé, Unité 756, Faculté de Pharmacie, Paris XI, Châtenay-Malabry, France

Running Title: Dr Adhesins bind independently to DAF and N-domain of CEA

Address correspondence to: Steve L. Moseley, Department of Microbiology, University of Washington, Box 357242, Seattle, WA 98195-7242. Telephone: 206-543-2820. Fax 206-543-8297. Email: moseley@u.washington.edu.

Escherichia coli expressing the Dr family of adhesins adhere to epithelial cells by binding to decay-accelerating factor (DAF) and carcinoembryonic antigen (CEA)-related cell surface proteins. The attachment of bacteria expressing Dr adhesins to DAF induces clustering of DAF around bacterial cells, and also recruitment of CEA - related cell adhesion molecules. CEA, CEACAM1, and CEACAM6 have been shown to serve as receptors for some Dr adhesins (AfaE-I, AfaE-III, DraE, and DaaE). We demonstrate that AfaE-I, AfaE-V, DraE, and DaaE adhesins bind to the N-domain of CEA. To identify the residues involved in the N-CEA/DraE interaction, we performed SPR binding analyses of naturally occurring variants and a number of randomly generated mutants in DraE and N-CEA. Additionally, we used chemical shift mapping by nuclear magnetic resonance (NMR) to determine the surface of DraE involved in N-CEA binding. These results show a distinct CEA binding site located primarily in the A, B, E and D strands of the Dr adhesin. Interestingly, this site is located opposite to the β -sheet encompassing the previously determined binding-site for DAF, which implies that the adhesin can bind simultaneously to both receptors on the epithelial cell surface. The recognition of CEACAMs from a highly diverse DrCEA subfamily of Dr adhesins indicates that interaction with these receptors plays an important role in niche adaptation of *E. coli* strains expressing Dr adhesins.

The Dr family of adhesins of *Escherichia coli* is associated with diarrhea and urinary tract infections (UTI), in particular, gestational pyelonephritis and recurring cystitis (1-3). This family includes AfaE-I, AfaE-II, AfaE-III, AfaE-V, Dr hemagglutinin (DraE), Dr-II, DaaE, and NfaE-I (4). Dr adhesins recognize as receptors decay-accelerating factor (DAF) and the DrCEA subfamily recognizes carcinoembryonic antigen (CEA) - related cell adhesion molecules (CEACAM) (5, 6). DAF is a complement regulatory protein present on a variety of epithelial surfaces, including gastrointestinal mucosa, exocrine glands, renal pelvis, ureter, bladder, cervix and uterine mucosa (7).

The CEACAM family is a group of highly glycosylated homotypic/heterotypic cell surface intracellular adhesion molecules which includes CEA, CEACAM1, CEACAM3, CEACAM4, CEACAM6, CEACAM7 and CEACAM8 (8). It has been reported recently that *E. coli* expressing some Dr adhesins, AfaE-I, AfaE-III, DraE, and DaaE (the DrCEA subfamily), adhered to CHO cells expressing CEA, and that *E. coli* expressing AfaE-III, DraE, and DaaE adhered to CHO cells expressing CEACAM1 and CEACAM6 (9). These adhesins also elicit the recruitment of CEACAM1, CEA, CEACAM6 and CEACAM3 to the sites of adherent bacteria (9). Recognition of CEA and CEACAM6 but not CEACAM1 is accompanied by tight attachment of the bacteria to elongated cell surface microvillus-like extensions. This cellular response results from activation of Rho

GTPase Cdc42 and phosphorylation of ezrin/radixin/moesin (ERM) (9).

The CEA family is a member of the immunoglobulin (Ig) superfamily (8, 10). Each CEA family member consists of an N-terminal Ig variable (IgV)-like domain. At the amino acid level, the N-terminal domain exhibits greater than 90% identity with other members of the CEA subgroup. The N-terminal domain may be followed by up to six IgC2 domains (A1, B1, A2, B2, A3, B3) (8), which are all present in CEA. CEACAM1, CEACAM3, CEACAM4 are inserted into cellular membrane via a carboxy-terminal transmembrane and cytoplasmic domain, while CEA, CEACAM6, CEACAM7, CEACAM8 are anchored to the membrane via GPI. These molecules are expressed on numerous cells including epithelial, endothelial and myeloid cells (11). Within the family, CEACAM1, a signaling receptor, is the most widely expressed in distinct human tissues, being present in granulocytes, monocytes and epithelial cells in different organs including colonic and respiratory epithelia (8, 12, 13).

It has been reported that *E. coli* and *Salmonella enterica* bind CEACAM molecules via their mannosyl residues (14-16). Several microorganisms including *Neisseria meningitidis*, *N. gonorrhoea*, *Haemophilus influenzae*, and *Moraxella catarrhalis* target members of the CEACAM family via the proteinaceous component of the N-terminal domain (17-22). *Neisseria* spp. bind CEACAM molecules via the structurally related Opa proteins, while in the case of *H. influenzae* and *M. catarrhalis* the ligands appear to be distinct from this family (22, 23). Targeting of CEACAM molecules by *Neisseria* leads to cellular invasion and passage across polarized monolayers (24).

In this study we provide evidence that DrCEA subfamily of adhesins, including AfaE-I, AfaE-III, AfaE-V, DraE, and DaaE, bind to the N-domain of CEA. Using a combined nuclear magnetic resonance (NMR) and mutagenesis approach we identified amino acids of Dr/Afa-III adhesins and CEA involved in the interactions. We demonstrate that Dr/CEA interaction is sensitive to Cm inhibition due to direct disruption of the CEA-binding surface of the adhesin. Using NMR we also show that CEA and DAF binding

sites do not overlap and that DAF does not inhibit binding to CEA.

EXPERIMENTAL PROCEDURES

Bacterial strains were grown in Luria-Bertani (LB) or Super Broth (SB) medium at 37°C. Derivatives of pUC-Cm were grown in the presence of 25 µg/ml chloramphenicol (Cm). Derivatives of pET-21d and pCC90-D54stop were grown in 100 µg/ml ampicillin (Amp) or carbenicillin. *E. coli* DH5α (Life Technologies, Inc., Rockville, Md.) and BL21 (DE3) (Novagen, San Diego, CA) were host for the plasmids. The purification of *E. coli* chromosomal DNA, plasmid isolation, *E. coli* transformation, restriction enzyme digestion or ligation were carried out as described (25). Enzymes were purchased from New England Biolabs (Beverly, Ma) and used as recommended by the manufacturer.

The Chinese hamster ovary (CHO) cell transfectant clones that express human CEA or the vector alone were used (9). Cells were cultured in Ham's F12 supplemented with 10% fetal bovine serum (FBS) and 400 µg/ml of hygromycin B, and cultured according to standard tissue culture techniques.

All constructs were confirmed by sequencing using Big Dye Terminator method and ABI sequencing (PE Applied Biosystems, Foster City, CA).

Cloning, expression and purification of N-domain of CEA, CEACAM1, CEACAM6, CEACAM8 and CEA-CEACAM8 chimera — The sequences corresponding to the mature amino acid sequence of N-domain of CEA, CEACAM1, CEACAM6, CEACAM8 were PCR amplified using cDNA clones (image ID:5184800, 4540619, 3640231, 4618311; ATCC) as templates and inserted into pET-21d (Novagen). The CEA-CEACAM8 chimera was synthesized using the PCR-based splicing by overlap extension using CEA and CEACAM8 cDNA clones as templates and the following oligonucleotide pairs: CEAF, 5'-ccatgccaagctcactattgaatc-3'; CEACAM8-CEAF, 5'-gattgctgtatgcaggccctgggtagctgttgagttc-3', and CEACAM8r, 5'-gaagcttttaagtctccggatgtacgctgaac-3'; CEA-CEACAM8f, 5'-gaactcaacaagctaccccaggcctgcatacagaatc-3'. The chimera was then amplified by adding CEAF and

CEACAM8r primers to the PCR mix. The hybrid molecule was cloned into pET-21d (Novagen). The proteins were expressed in *E. coli* BL21 (DE3) and purified from inclusion bodies. The inclusion bodies were dissolved overnight in buffer containing 30 mM Tris/HCl (pH 8.5), 150 mM NaCl, 1 mM EDTA and 8 M urea. One volume of the protein sample was added slowly to 20 volumes of buffer containing 50 mM CHES (pH 9.2) and 500 mM arginine, and the sample was left overnight at 4 °C. The refolded protein was concentrated by ultrafiltration and purified by gel-filtration using a Superdex 75 column (Amersham Corporation, Piscataway, N.J) in 30 mM Tris/HCl (pH 8.5), 150 mM NaCl. Calibration of the column was performed using gel filtration markers (Amersham).

Purification of CEA N-A3 domain — CEA containing N and A3 domains and an oligohistidine tag at the N-terminal end (CEA N-A3) was expressed in *Pichia pastoris* as described in (26) (*P. pastoris* strain generously provided by Dr. John E. Shively, Beckman Research Institute City of Hope, Duarte, CA). CEA N-A3 was purified from the supernatant of induced cultures by Ni-NTA chromatography as described previously (26, 27). For SPR experiments, the protein was then purified by gel filtration chromatography using a Superdex 200 column (Amersham) in HBS-E buffer (10 mM HEPES [pH 7.4], 150 mM NaCl, 3 mM EDTA).

Purification of Dr family fimbriae — Genes encoding Dr adhesins were amplified by using the following primers: for DraE and AfaE-III: DraE-BamHI, ggatccgaaggagatatacatatgaaaaaattagcgatcatggcc, and DraE-PstI, cacgcacgtcctgcagtcattttgccagtaacc; for AfaE-V: DraE-BamHI primer and AfaE-V-PstI, cacgcacgtgcagtcaactcaccagtagcccccagt; for NfaE: NfaE-BamHI, cgaggatccgaaggagatatacatatgaaaataaaatatacatgatg, and NfaE-PstI, cacgcacgtgcagttattggctgtacactgccc. Products were digested with *BamHI* and *PstI* and inserted into *BamHI* and *PstI* restriction sites of pUC-Cm. Gene encoding DaaE adhesin was amplified by using the following primers: DaaE-BamHI, cgatccgaacaggtaatcaatatagaaaaattagcgataatg and DaaE-EcoRI, gaattcttagtctgcagtaacccc. Product was digested with *BamHI* and *EcoRI* and inserted

into *BamHI* and *EcoRI* restriction sites of pUC-Cm. Gene encoding AfaE-I adhesin was amplified by using the following primers: AfaE-I-EcoRI, gaattcgaaggagatatacatatgaaaaaattagcgatcatag, and AfaE-I-PstI, cacgcacgtgcagttattttgtccagaacccgcttcg. Product was digested with *EcoRI* and *PstI* and inserted into *EcoRI* and *PstI* restriction sites of pUC-Cm. The resulting plasmids were transformed into *E. coli* 191A (pCC90-D54stop). This strain contains the necessary genes of the *dra* operon for fimbrial expression, with a premature stop codon at codon 54 within *draE*. Dr fimbriae were purified from recombinant strains as described previously (28). For SPR analysis, fimbriae were purified by gel filtration chromatography using a Superdex 200 column (Amersham) in HBS-E buffer.

Purification of DAF — DAF₂₃₄ contains short consensus repeats 2, 3, and 4 and an oligohistidine tag at the C-terminal end and was purified from recombinant *P. pastoris* kindly provided by Susan Lea, Oxford University, as previously described (29).

Surface plasmon resonance studies — SPR measurements were carried out in HBS-EP buffer (10 mM HEPES [pH 7.4], 150 mM NaCl, 3 mM EDTA, 0.005% P-20 surfactant [BIAcore AB, Uppsala, Sweden]) using a BIAcore 2000 system (BIAcore AB). To analyze the interaction between Dr fimbriae and N-domains of CEACAM receptors, native fimbriae were immobilized on a CM5 research-grade sensor chip (BIAcore AB) by amine coupling chemistry using the manufacturer's protocols. Immobilization of 500 response units (RU) resulted in optimal responses. The N-domain of each CEACAM was dissolved in running buffer and analyzed using a ~10² dilution series, i.e., (3-300 μM). Analyte was injected over the surface at a flow rate of 20 μl/min for 2 min. For competition experiments, DAF₂₃₄ (30 μM final concentration), or Cm (1 mM final concentration) were added to the running buffer. The affinities of the interactions were studied under steady-state conditions. Average equilibrium responses were measured for six to seven concentrations of CEACAM receptor. Raw sensorgrams were corrected using the double-subtraction protocol (30) and by subtracting both the reference flow cell response and the average of eight buffer injections. The resulting data were analyzed with

BIAevaluation 3.0 software (BIAcore AB) to globally fit the data and derive equilibrium constants describing the intermolecular interactions. The reported K_D values are the average of at least three independent experiments. Error estimates were propagated from the standard error (SE) of the association constant (K_A).

Chemical shift mapping for the AfaE-dsc and N-CEA interaction—The recombinant *E. coli* strain expressing AfaE-III-dsc has been described previously (31). An ^{15}N -labelled sample of AfaE-III-dsc was produced in minimal media, containing 0.07% $^{15}\text{NH}_4\text{Cl}$ and 0.2% C-glucose, supplemented with 50 $\mu\text{g/ml}$ Amp. AfaE-III-dsc was purified under denaturing conditions using the binding of the N-terminal hexahistidine tag to Nickel-bound agarose beads as described previously (31). Purified protein was refolded by dialysis into 50 mM sodium acetate buffer, pH 5.0 and concentrated to approximately 0.2 mM for NMR. N-CEA in the same buffer was introduced at several molar ratios until saturation was achieved and 2D ^{15}N - ^1H HSQC experiments were recorded at each stage under identical experimental conditions. ^1H - ^{15}N resonances shift changes and line widths were monitored by analysis of the 2D ^1H - ^{15}N HSQC spectra.

PCR mutagenesis of DraE — DraE was subjected to PCR mutagenesis using the GeneMorph II Random Mutagenesis Kit as directed by the manufacturer (Stratagene, La Jolla, CA) The pCC90 vector containing *draE* (32) was used as a template with following primers: 5ranmut, 5'-cccgccgccgattcgggtaagacagc-3' and 3ranmut, 5'-cccgccgccctgcagtcatttggcccagtaacc-3'.

Transformants containing mutant derivatives of *draE* were constructed as described previously (28).

Selection for CEA-binding deficient mutants — CEA N-A3 protein was used to coat seven 6-well microtiter plates at a concentration of 5 $\mu\text{g/ml}$ in bicarbonate buffer at 37°C for 1 h. Anti-Dr rabbit antisera (32) was dissolved in bicarbonate buffer at a 1:100 dilution and used to coat 6-well microtiter plates at 37 °C for 1 h. The wells were blocked with 0.01 M phosphate-buffered saline pH 7.2 (PBS) containing 1% BSA for 15 min at 37 °C. Transformants containing the mutant *draE* derivatives were resuspended in 12 ml of PBS to an OD_{540} of 0.025. 2 ml of cell suspension were

added to each well coated with CEA and allowed to bind for 45 min at 37 °C. The supernatant containing unbound bacteria was collected and added to a fresh plate coated with CEA. These steps were repeated successively for a total 6 times. The final supernatant was added to a microtiter plate coated with anti-Dr antisera and allowed to bind for 45 min at 37 °C. The unbound bacteria were removed by 7-9 washes with PBS and 2 ml of SB medium were added to each well. The plate was incubated with shaking at 37 °C for 1 h. The resulting bacterial suspension was plated on LB medium containing Amp, Cm and X-gal. White colonies were selected and examined for erythrocyte binding by a mannose-resistant hemagglutination assay (MRHA, see below). Those transformants that were MRHA⁺ were analyzed for CEA binding.

Mannose resistant hemagglutination assay (MRHA) — MRHA with human erythrocytes of blood group O was performed as previously described (28).

CEA binding growth assay — Those transformants that were MRHA⁺ were examined for the ability to bind CEA. CEA N-A3 was used to coat 96-well microtiter plates as described above. 100 μl of an overnight culture of each transformant, $\text{OD}_{540} = 4.0$, were added to individual wells and allowed to bind for 45 min at 37 °C. The unbound bacteria were removed with PBS then 150 μl of SB medium were added to each well. The plate was incubated with shaking at 37 °C for 2 h. The resulting growth was then measured at OD_{540} . Those transformants that exhibited little or no growth were further analyzed to confirm DraE expression.

Surface expression assay and sequencing analysis of mutants — To confirm that the transformants express the various mutant adhesin variants at equivalent levels, they were examined for the ability to bind polyclonal antisera prepared against DraE (32). This assay was performed in the same manner as the CEA binding growth assay with following modification. Plates were coated with anti-Dr antisera at a 1:200 dilution for 2 hours. Those transformants that exhibited growth were selected for sequencing.

CEA binding assay with radiolabeled bacteria — This assay was performed in the same manner as the CEA binding growth assay with the following modifications. Plates were coated with soluble CEA (Xema, Moscow, Russia) or CEA N-A3 at a concentration of 15, 10, 5 and 3 µg/ml in PBS. The bacterial strains were grown overnight in SB supplemented with 10 µCi/ml of ³H-thymidine at 37 °C. The cells were then pelleted and resuspended in PBS and adjusted to OD₅₄₀ = 4.0. 50 µl of each of the bacterial strain suspensions were added to a microtiter plate well together with 50 µl of PBS containing 0.2% BSA and allowed to bind for 1 hour at 37 °C. To test the effect of competitors (DAF₂₃₄, N-domain of CEA, and Cm) on bacterial binding to CEA, 20 µM of N-domain of CEA, 80 µM DAF, or 10 mM Cm were added to PBS containing 0.2% BSA. Unbound bacteria were removed by washing with PBS and the wells were dried at 60 °C. The wells were placed in scintillation fluid and bound bacteria quantified by scintillation counting.

Site-directed mutagenesis of CEA gene — Mutations were introduced into the CEA (N-domain) gene on plasmid pET-21d (this study) by site-directed mutagenesis using the Quick Change Kit as directed by the manufacturer (Stratagene). Constructs containing mutations were identified by sequence analysis.

CHO cell-binding assay — CHO cells were split into 24-well plates with glass coverslips and grown to confluence. Before the assay, cells were washed twice with Hanks' balanced saline solution (HBSS) and incubated with fresh medium without antibiotics and without FBS for 1 h. The bacterial strains were grown overnight on LB medium and harvested and resuspended in PBS to OD₅₄₀ = 0.6. The bacterial cells were pelleted and resuspended in the tissue culture medium. Then 0.1 ml of each bacterial strain were added to each well. The adherence assay was performed as described previously (28) and repeated in triplicate.

RESULTS

Adhesins of the DrCEA subfamily, including AfaE-I, AfaE-V, DraE, and DaaE bind soluble CEA, CEA N-A3 and CHO cells expressing CEA — Previously it has been shown that Dr adhesins including DraE, AfaE-III and DaaE bind and elicit

recruitment of CEA, CEACAM1 and CEACAM6 (9). To determine if other members of Dr family can bind CEA, recombinant *E. coli* expressing different Dr adhesins were constructed. Dr adhesins were expressed in a background strain containing a mutant *dra* operon expressing genes necessary for assembly of the Dr fimbriae, but not the adhesin itself. Transfected CHO cell lines expressing human recombinant CEA or containing the expression vector alone were used to study the recognition of CEA by bacteria expressing Dr adhesins. None of the tested strains showed binding to CHO cells containing the vector alone. Strains expressing DraE/AfaE-III alleles, DaaE, and AfaE-V were able to bind 60-80% of CHO-CEA cells, whereas the parent strain with a premature stop codon in *draE* did not bind the cells. The recombinants expressing AfaE-I demonstrated poor binding to CHO-CEA cells, while *E. coli* expressing NfaE did not mediate adherence to this cell line.

To further investigate the CEA-binding phenotype of Dr adhesins, we coated plates with soluble CEA (15, 10, 5, and 3 mg/ml) and incubated them with radiolabelled *E. coli* expressing the adhesins. Strains expressing DraE, DaaE, and AfaE-V adhered strongly to plates coated with CEA at all tested concentrations (Fig. 1). Moreover, these strains also bound to a CEA derivative construct consisting of only the N and A3 domains (data not shown).

Previously observed phenotypes of AfaE-I and NfaE correlated well with the ability of the recombinants to bind to CEA-coated plates (Fig. 1). NfaE did not mediate bacterial binding to CEA and CEA N-A3 plates. When bacteria expressing AfaE-I were incubated with the plates coated with 15 and 10 mg of CEA, this adhesin demonstrated a level of adherence comparable to DraE, DaaE and AfaE-V. However, AfaE-I mediated a reduced level of binding to plates coated with CEA at a concentration of 5 mg/ml and failed to bind CEA at 3 µg/ml. These data indicate that the affinity of AfaE-I for CEA is significantly lower than DraE, DaaE or AfaE-V, but as multiple adhesin subunits contribute an avidity effect to the interaction, their binding can only be compared at low concentrations of CEA. Taken together, these results demonstrate that recognition of CEA is expressed by most adhesins of Dr family and N-

terminal and A3 domains are sufficient for these interactions.

The N-terminal domain of CEA mediates binding to AfaE-I, AfaE-III, AfaE-V, DraE and DaaE — Dr adhesins recognize as receptors CEA, CEACAM1 and CEACAM6 and also elicit the recruitment of CEACAM3 around adhering bacteria (9). Since the N-terminal and A3 domains of CEA are sufficient for bacterial adherence and the N-terminal domains of CEACAMs have high sequence similarity (Fig. 2A), we hypothesized that the N-domain of CEA, CEACAM1 and CEACAM6 is the target for Dr adhesins. To test our hypothesis we constructed *E. coli* recombinants expressing the N-domain of CEA (N-CEA), and isolated the protein from inclusion bodies. In a similar manner, the N-domain of CEACAM8 (N-CEACAM8) was cloned, expressed and purified. When N-CEA was tested as an inhibitor in the CEA binding assay with radiolabeled strains expressing DraE and AfaE-III adhesins, bacterial adherence was inhibited significantly, suggesting that the adhesins recognize the N-domain on CEA (Fig. 2B).

We examined the affinity of Dr adhesins (AfaE-I, AfaE-III, AfaE-V, DraE, DaaE, and NfaE) to N-CEA and N-CEACAM8 by surface plasmon resonance (SPR) analysis. N-CEACAM8 has a high sequence similarity with N-CEA (Fig. 2A) but CHO cells expressing CEACAM8 are not recognized by Dr adhesins (9). The affinities of the interactions were studied by immobilizing purified adhesin to the sensor surface and flowing CEACAMs over the surface. No change in the resonance signal was detectable when N-CEACAM8 was injected to flow over adhesin-immobilized sensor surface, indicating the absence of detectable binding. No binding was observed when NfaE was immobilized to the sensor surface and N-CEA was used as analyte.

SPR studies indicated that the interactions between AfaE-I, AfaE-III, AfaE-V, DraE, and DaaE adhesins and N-CEA are characterized by very fast on and off rates, therefore steady-state conditions were used to calculate affinity (Fig. 3A). Interestingly, AfaE-V, which does not mediate MRHA and displays very low affinity to DAF (unpublished observations), was the strongest binding variant among the tested adhesins. AfaE-I demonstrated the lowest affinity

to N-CEA, consistent with previously observed phenotype (Fig. 3B).

Effect of competitors (Cm and DAF) on AfaE-III and DraE binding to CEA — It has been shown that the binding of DAF to DraE is inhibited by chloramphenicol (Cm) (3). However, adherence of DAF to AfaE-III, differing from DraE by three non-synonymous nucleotide changes (D52N, T88M, I111T), is resistant to Cm (3). X-ray studies of DraE in complex with Cm indicated that Cm interacts with P40, G42, P43, I111, G113, I114 and Y115 of DraE, and Cm sensitivity of DraE is caused by direct disruption of DAF-binding surface of the adhesin (33). To investigate the effect of Cm on DraE/CEA interactions, bacterial cells expressing DraE or AfaE-III were mixed with 15 mM Cm and incubated with CEA-coated plates (Fig. 2B). Binding of DraE-expressing bacteria was inhibited by Cm, while AfaE-III-expressing *E. coli* were resistant to Cm inhibition (Fig. 2B). These data suggest that DraE binding to Cm disrupts the CEA-binding surface of the adhesin.

Amino acids involved in DAF/AfaE-III and DAF/DraE interactions were implicated by mutagenesis and NMR studies (28, 31). NMR analysis has suggested that the DAF binding region of AfaE-III involves a large surface comprising domains A1, A2, B, C2, E, F and Gd (31). To determine if binding of DraE adhesins to DAF disrupts the CEA-binding surface of the adhesin, DAF₂₃₄ was tested as a competitor in the CEA-binding assay with radiolabeled bacteria. DAF had no effect on bacterial adherence to the CEA-coated plates, implying that the binding domains for DAF and CEA are distinct (Fig. 2B).

In order to confirm with the effect of DAF or Cm on binding of N-domain of CEA to fimbrial preparations, we utilized SPR analysis. DAF₂₃₄ (30 μ M) or Cm (1 mM) was added to buffer containing N-CEA, and flowed over DraE fimbriae immobilized on the sensor surface. Results are clearly consistent with the CEA binding assay with DraE-expressing bacteria described above. DAF had no effect on the affinity of DraE for N-CEA ($K_D=13.1\pm 1.5$ μ M). However when DAF was replaced with Cm (1 mM), N-CEA failed to bind the DraE immobilized surface.

Analysis of CEA binding phenotypes of DraE/AfaE-III clinical isolates — To investigate the functional variability of DraE/AfaE-III alleles with regard to CEA binding, we purified naturally occurring DraE-related fimbrial variants and utilized SPR to determine the affinity to N-CEA as described above. We found that three variants, JJB17, 2099 and 293 had low affinity to N-CEA (Fig. 4A). JJB17 and 293 each differ from DraE by a single non-synonymous mutation, I111T and T88A, respectively. 2099 differs from JJB17 by one mutation, D61G.

Four adhesins, 513, G2076, 252 and 297, have increased affinity to N-CEA (Fig. 4A). 513 and 297 differ from DraE by single non-synonymous mutations, T88M and I85M, respectively. G2076 differs from 513 by one mutation, G68D. 252 differs from DraE by two non-synonymous mutations, A92T and I111V. Interestingly, AfaE-III, differing from 513 by two non-synonymous nucleotide changes (D52N, I111T) demonstrated N-CEA affinity comparable to DraE. This adhesin acquired two CEA-binding mutations, T88M and I111T. It is possible that the positive effect of the T88M mutation on CEA binding compensates the negative effect of I111T mutation. Thus, our data suggest that: (i) residues I111, T88 and I85 are important for DraE/N-CEA interactions; (ii) the DraE sub-group accumulates a high number of non-synonymous substitutions leading to variation in CEA-binding phenotypes of the adhesins.

Identification of amino acids of DraE involved in CEA binding by random mutagenesis — To independently identify amino acids of the adhesin critical for recognition of CEA and provide further evidence for our NMR-derived N-CEA binding surface, we performed random mutagenesis of DraE. Several mutant strains were isolated that mediated MRHA but demonstrated very weak binding to CEA-coated plates. We chose to further characterize 6 mutants that contained single amino acid substitutions within DraE (P40S, P43V, R86G, G113A, Y115F, Y115A).

To examine the effect of the mutations in DraE upon its binding properties, fimbriae were isolated from the bacterial mutants. The affinities of DraE/CEA interactions were analyzed by SPR as described above. Figure 4,B summarizes the DraE mutations and their effects on CEA binding. All mutants mediated binding to N-CEA, but the

mutations significantly weaken the interactions between DraE and CEA. The mutation at positions R86G has the largest effect, decreasing the affinity more than seven fold. The position of DraE mutations affecting CEA binding are shown in Figs. 5B, 6A and 6C.

Identification of binding site for CEA in Dr adhesin by NMR chemical shift mapping — Our earlier work on the structure and assembly of the Dr adhesins provides further opportunity to perform NMR titration experiments to directly investigate the binding site for CEA (31). An analysis of amide line-width and chemical shift changes for AfaE-III-*dsc* in the presence of N-CEA was carried out (Fig. 5A). The CEA binding region of AfaE-III-*dsc* may be delineated, and lies entirely on one side of the molecule, forming a surface comprising side-chains from principal strands A1, B, E, D and adjacent loop regions (Fig. 5B,C, Fig. 6E,F). Key amides perturbed in the presence of N-CEA include G6, K12, Q20-G24, I41, G42, V44-L49, R54-V56, A60, G68, F70, M88, S91, A92, N97, D104, G106, W108, G110-I112, I114, and A138.

Identification of amino acids of CEA involved in Dr adhesin binding — To investigate the affinity of DraE to other members of CEACAM family we constructed *E. coli* recombinant expressing N-domains of CEACAM1 (N-CEACAM1) and CEACAM6 (N-CEACAM6). N-CEACAM1 affinity for DraE was comparable to N-CEA (Table 1). However, N-CEACAM6 showed weak binding to the adhesin. DraE does not interact with N-CEACAM8, as discussed above. Sequence alignment of the N-domains of CEACAM-related proteins, including CEACAM1, CEACAM3, CEA, CEACAM6, and CEACAM8 revealed exceptional homology (Fig. 2A). In order to identify amino acids of CEA N domains involved in CEA/Dr interactions we constructed a CEA-CEACAM8 chimera consisting of the residues 1-58 of the N domain of CEA fused to residues (59-110) of the CEACAM8 N-domain and analysed the ability of the chimeric protein to bind DraE by SPR. We found that the affinities obtained for wild-type and the mutant were the same (Table 1) implying that the N-terminal 58 amino acids of CEA are crucial for the CEA/DraE interaction.

Using homologue scanning mutagenesis of the N-terminal 58 amino acids of CEA, we replaced single residues of CEA with

corresponding residues of CEACAM8 and determined the affinity of the mutants to DraE. As is shown in Table 1, mutations in F9, V11, L28, S32, V39, G51 and T52 had no significant effect on DraE/N-CEA interactions. Mutation D40A caused an almost four fold drop in the DraE/N-CEA affinity and two mutations, F29R and Q44R, abolished the interaction.

DISCUSSION

Diffusely adhering *Escherichia coli* (DAEC) strains express adhesins of Dr family and cause symptomatic urinary tract or intestinal infections (4). The Dr family of adhesins is comprised of a number of related adhesins with extensive sequence diversity. This variability of Dr adhesins is emerging under strong positive selection and results in the generation of clades within the family, and the accumulation of point mutations within the clades (Korotkova et al., manuscript submitted). Variability in the Dr family of adhesins results in functional diversity with regard to receptor specificity (9, 32).

E. coli expressing Dr adhesins adhere to human cells by recognition of the brush border-associated DAF (4). The attachment of bacteria expressing AfaE-III, DraE, and DaaE to DAF induces clustering of DAF around bacterial cells, and also recruitment of the brush border proteins, CEA, CEACAM1, CEACAM3 and CEACAM6 (6, 9). It has been shown that Dr adhesins including AfaE-III, DraE, and DaaE are involved in adherence to CEA, CEACAM1 and CEACAM6, thus indicating that these molecules might be important for DAEC colonization (9).

In this study we have demonstrated that the bacteria expressing AfaE-I, DraE/AfaE-III alleles, AfaE-V, and DaaE recognize the N-domain of CEA. Thus, these studies add to the list of bacterial ligands that target the N-domain of CEA. Adherence to this receptor by apparently structurally distinct proteins of several bacterial genera points to the importance of CEA for the colonization of pathogens.

We found that the DraE adhesin also recognizes the N-domains of CEACAM1 and CEACAM6, demonstrating low affinity to CEACAM6 and high affinity to CEACAM1. Homology scanning mutagenesis of N-CEA revealed that F29 and Q44 (and to a lesser extent

D40) of CEA are required for maximal DraE binding affinity. These residues are located in the exposed loops of the GFCC'C" face of the CEA N-domain, which is not sheltered by carbohydrate as revealed by crystal structure of murine CEACAM1 (34, 35) and would be accessible for pathogen binding (Fig 5,D). The solvent exposed area around F29 in CEA is hydrophobic and might be important for contacts with Dr adhesins. It has been shown that other pathogenic bacteria also target this exposed protein face of the N-terminal IgV-like domain of CEACAM receptors (18-20, 36).

CEACAM family members can exist as dimers in the plasma membrane of eukaryotic cells, and recombinant N domains of CEA have been shown to form oligomers in solution (37-39). It has also been demonstrated that residues on the GFCC'C" face of the CEA, are directly engaged in homophilic cell adhesion (34, 40). Notably, amino acid residues V39A, D40 and Q44 in CEACAM1 have been reported to play an important role in homophilic cell adhesion of CEACAM1 (41, 42), which suggests that DraE binding to CEA at least partly overlaps the dimerization surface and therefore is likely to inhibit the CEA homophilic interaction. Structural studies of the CEA-DraE complex are needed to provide detailed information about the mechanism of DraE recognition of the receptor.

Using the recently published NMR and X-ray structures of AfaE/DraE (pdb 1RXL and IUSQ (31, 33)) we have identified the N-CEA binding-site on the DraE surface. NMR chemical shift mapping and line-width analysis of backbone amides define a contiguous patch of residues in strands A1, B, E, D and neighboring loop regions. Furthermore, random mutagenesis and functional analyses of the DraE/AfaE-III alleles identified residues P40, P43, R86, I85, T88, I111, G113, and Y115 as important for binding to CEA. Figure 6 illustrates the surfaces mapped by the different approaches. In NMR chemical shift mapping, contiguous stretches of perturbed amide delineate the likely binding surface. The presence of proline residues and overlapped resonances can cause an underreporting, while indirect perturbations highlight regions outside the binding interface. Care should also be taken when interpreting mutagenesis experiments, as meaningful substitutions must not severely affect protein

stability. The combined use of NMR mapping and mutagenesis provides a powerful and robust approach for identifying protein-protein interfaces. As shown in Figure 6, the CEA binding region defined by mutagenesis clearly overlaps with that determined by NMR experiments. The mutation-derived and NMR-derived surfaces are on the same face of the molecule and in proximity to the Cm binding pocket, which is consistent with the discovery that Cm inhibits CEA binding by DraE. DAF/DraE interactions are also sensitive to the presence of Cm, and therefore one might expect that DraE binding to CEA would be inhibited by DAF. However, our data demonstrate that DAF has no inhibitory effect on CEA/DraE interactions, implying that the adhesin can simultaneously bind both receptors on the host tissue. Combined mutation and NMR-derived interaction surface for DAF and CEA are mutually exclusive and thus consistent with the inability of DAF to inhibit CEA binding.

Previously it has been shown that DraE mutations at positions T88 and I111 affect type IV collagen binding of the adhesin (32). According to our unpublished observations, the amino acids P40, P43, I114, Y115 are also important for DraE/collagen interactions. Mutations P40A, P43V, I114A and Y115A resulted in a complete loss of recognition of collagen by DraE. Therefore, the hydrophobic surface on DraE that includes these residues is involved in the binding of three molecules, CEA, Cm and the 7S domain of type IV collagen.

Dr adhesin-expressing *E. coli* penetrate into epithelial cells utilizing a zipper-like mechanism of internalization (43), although neither the mechanism of internalization nor the roles of specific binding activities of Dr adhesins in internalization have been defined in detail. Apart from the interactions of the Dr adhesins, it has been shown that the Dr invasin (afaD-related proteins) contribute to the process of internalization (44-47). DAF is concentrated in lipid rafts (43), cell surface invaginations that are believed to be important for signal-transduction (48). We hypothesize that the role for DAF in Dr-mediated infection is to promote initial binding to the cell membrane. This hypothesis is supported by the observation that all adhesins of the Dr

family bind DAF (4), and that DraE-family alleles are adapting to the uropathogenic niche by strong positive selection for mutations in the adhesin that enhance binding to DAF (Korotkova et al, manuscript submitted). Bacterial binding to DAF is followed by sequential recruitment of adjacent GPI-anchored receptors, such as CEA and CEACAM6, the carboxy-terminal transmembrane-anchored CEACAM1 and CEACAM3, and interactions with surface structures such as β 1 integrins that participate in internalization and/or signalling events (6, 43).

The role of CEACAMs in *E. coli* infection mediated by Dr adhesins is not yet clear. However, the occurrence of point mutations in Dr adhesins which affect CEACAM binding, under positive selection, and at high frequency, suggests that CEACAMs receptors play an important role in niche adaptation of *E. coli*. It has been shown that CEACAMs receptors are involved in *N. gonorrhoeae* internalization by epithelial cells (49). Moreover, CEA and CEACAM6 mediate zipper-like internalization of *N. gonorrhoeae* (49). We suggest that these receptors might have similar function during *E. coli* colonization, providing tight association between bacteria and cell membrane which ultimately results in the envelopment of the bacterial body by the cell membrane and sequential bacterial uptake through a zipper-like process.

The ability of DraE to interact simultaneously with two receptors is an intriguing observation. The presence of two distinct receptor binding sites on the adhesin could be the result of two independent evolution processes directed toward preserving both activities. Genetic adaptation to one environment is often associated with loss of fitness in other environments. If the binding sites for two receptors overlap, positive selection associated with the adaptation to the first receptor might lead to the loss of binding to the second receptor. Independent receptor binding sites may be important for Dr-mediated *E. coli* persistence in the host environment because they would contribute to the maintenance of lipid raft integrity and provide multiple high affinity interactions that can lead to bacterial internalization.

Table. 1. Affinity (K_D) of DraE adhesin to N-CEACAMs and N-CEA mutants

N-domains of CEACAMs and N-CEA mutants	K_D , μM
N-CEA	13.1 \pm 2.5
N-CEACAM1	15.3 \pm 3.8
N-CEACAM6	30.1 \pm 2.8
CEA-CEACAM8 chimera	14.4 \pm 2.1
F9A	18.4 \pm 1.5
V11A	24.9 \pm 1.2
L28P	6.6 \pm 0.5
F29R	>200
S32N	12.8 \pm 1.3
V39A	9.35 \pm 1.3
D40A	48.9 \pm 3.1
Q44R	>200
G51D	12.0 \pm 1.4
T52N	11.0 \pm 2.1

REFERENCES

1. Garcia, M. I., Gounon, P., Courcoux, P., Labigne, A. & Le Bouguenec, C. (1996) *Mol Microbiol* **19**, 683-93.
2. Foxman, B., Zhang, L., Tallman, P., Palin, K., Rode, C., Bloch, C., Gillespie, B. & Marrs, C. F. (1995) *J Infect Dis* **172**, 1536-41.
3. Nowicki, B., Labigne, A., Moseley, S., Hull, R., Hull, S. & Moulds, J. (1990) *Infect Immun* **58**, 279-81.
4. Servin, A. L. (2005) *Clin Microbiol Rev* **18**, 264-92.
5. Nowicki, B., Moulds, J., Hull, R. & Hull, S. (1988) *Infect Immun* **56**, 1057-60.
6. Guignot, J., Peiffer, I., Bernet-Camard, M. F., Lublin, D. M., Carnoy, C., Moseley, S. L. & Servin, A. L. (2000) *Infect Immun* **68**, 3554-63.
7. Medof, M. E., Walter, E. I., Rutgers, J. L., Knowles, D. M. & Nussenzweig, V. (1987) *J Exp Med* **165**, 848-64.
8. Hammarstrom, S. (1999) *Semin Cancer Biol* **9**, 67-81.
9. Berger, C. N., Billker, O., Meyer, T. F., Servin, A. L. & Kansau, I. (2004) *Mol Microbiol* **52**, 963-83.
10. Obrink, B. (1997) *Curr Opin Cell Biol* **9**, 616-26.
11. Prall, F., Nollau, P., Neumaier, M., Haubeck, H. D., Drzeniek, Z., Helmchen, U., Loning, T. & Wagener, C. (1996) *J Histochem Cytochem* **44**, 35-41.
12. Kodera, Y., Isobe, K., Yamauchi, M., Satta, T., Hasegawa, T., Oikawa, S., Kondoh, K., Akiyama, S., Itoh, K., Nakashima, I. & et al. (1993) *Br J Cancer* **68**, 130-6.
13. Metze, D., Bhardwaj, R., Amann, U., Eades-Perner, A. M., Neumaier, M., Wagener, C., Jantscheff, P., Grunert, F. & Luger, T. A. (1996) *J Invest Dermatol* **106**, 64-9.
14. Leusch, H. G., Drzeniek, Z., Markos-Pusztai, Z. & Wagener, C. (1991) *Infect Immun* **59**, 2051-7.
15. Sauter, S. L., Rutherford, S. M., Wagener, C., Shively, J. E. & Hefta, S. A. (1991) *Infect Immun* **59**, 2485-93.
16. Sauter, S. L., Rutherford, S. M., Wagener, C., Shively, J. E. & Hefta, S. A. (1993) *J Biol Chem* **268**, 15510-6.
17. Virji, M., Watt, S. M., Barker, S., Makepeace, K. & Doyonnas, R. (1996) *Mol Microbiol* **22**, 929-39.
18. Virji, M., Evans, D., Hadfield, A., Grunert, F., Teixeira, A. M. & Watt, S. M. (1999) *Mol Microbiol* **34**, 538-51.
19. Virji, M., Evans, D., Griffith, J., Hill, D., Serino, L., Hadfield, A. & Watt, S. M. (2000) *Mol Microbiol* **36**, 784-95.
20. Bos, M. P., Kuroki, M., Krop-Watorek, A., Hogan, D. & Belland, R. J. (1998) *Proc Natl Acad Sci U S A* **95**, 9584-9.
21. Toleman, M., Aho, E. & Virji, M. (2001) *Cell Microbiol* **3**, 33-44.
22. Hill, D. J. & Virji, M. (2003) *Mol Microbiol* **48**, 117-29.
23. Hill, D. J., Toleman, M. A., Evans, D. J., Villullas, S., Van Alphen, L. & Virji, M. (2001) *Mol Microbiol* **39**, 850-62.
24. Gray-Owen, S. D. (2003) *Scand J Infect Dis* **35**, 614-8.
25. Maniatis, T. (1982) *Molecular cloning : a laboratory manual* (Cold Spring Harbor Laboratory, Cold Spring Harbor, N.Y.).
26. You, Y. H., Hefta, L. J., Yazaki, P. J., Wu, A. M. & Shively, J. E. (1998) *Anticancer Res* **18**, 3193-201.
27. Hellwig, S., Robin, F., Drossard, J., Raven, N. P., Vaquero-Martin, C., Shively, J. E. & Fischer, R. (1999) *Biotechnol Appl Biochem* **30 (Pt 3)**, 267-75.

28. Van Loy, C. P., Sokurenko, E. V., Samudrala, R. & Moseley, S. L. (2002) *Mol Microbiol* **45**, 439-52.
29. Powell, R. M., Ward, T., Evans, D. J. & Almond, J. W. (1997) *J Virol* **71**, 9306-12.
30. Myszka, D. G. (1999) *J Mol Recognit* **12**, 279-84.
31. Anderson, K. L., Billington, J., Pettigrew, D., Cota, E., Simpson, P., Roversi, P., Chen, H. A., Urvil, P., du Merle, L., Barlow, P. N., Medof, M. E., Smith, R. A., Nowicki, B., Le Bouguenec, C., Lea, S. M. & Matthews, S. (2004) *Mol Cell* **15**, 647-57.
32. Carnoy, C. & Moseley, S. L. (1997) *Mol Microbiol* **23**, 365-79.
33. Pettigrew, D., Anderson, K. L., Billington, J., Cota, E., Simpson, P., Urvil, P., Rabuzin, F., Roversi, P., Nowicki, B., du Merle, L., Le Bouguenec, C., Matthews, S. & Lea, S. M. (2004) *J Biol Chem* **279**, 46851-7.
34. Tan, K., Zelus, B. D., Meijers, R., Liu, J. H., Bergelson, J. M., Duke, N., Zhang, R., Joachimiak, A., Holmes, K. V. & Wang, J. H. (2002) *Embo J* **21**, 2076-86.
35. Boehm, M. K., Mayans, M. O., Thornton, J. D., Begent, R. H., Keep, P. A. & Perkins, S. J. (1996) *J Mol Biol* **259**, 718-36.
36. Bos, M. P., Hogan, D. & Belland, R. J. (1999) *J Exp Med* **190**, 331-40.
37. Hefta, L. J., Chen, F. S., Ronk, M., Sauter, S. L., Sarin, V., Oikawa, S., Nakazato, H., Hefta, S. & Shively, J. E. (1992) *Cancer Res* **52**, 5647-55.
38. Hunter, I., Sawa, H., Edlund, M. & Obrink, B. (1996) *Biochem J* **320** (Pt 3), 847-53.
39. Krop-Watorek, A., Oikawa, S., Oyama, Y. & Nakazato, H. (1998) *Biochem Biophys Res Commun* **242**, 79-83.
40. Taheri, M., Saragovi, U., Fuks, A., Makkerh, J., Mort, J. & Stanners, C. P. (2000) *J Biol Chem* **275**, 26935-43.
41. Markel, G., Gruda, R., Achdout, H., Katz, G., Nechama, M., Blumberg, R. S., Kammerer, R., Zimmermann, W. & Mandelboim, O. (2004) *J Immunol* **173**, 3732-9.
42. Watt, S. M., Teixeira, A. M., Zhou, G. Q., Doyonnas, R., Zhang, Y., Grunert, F., Blumberg, R. S., Kuroki, M., Skubitz, K. M. & Bates, P. A. (2001) *Blood* **98**, 1469-79.
43. Kansau, I., Berger, C., Hospital, M., Amsellem, R., Nicolas, V., Servin, A. L. & Bernet-Camard, M. F. (2004) *Infect Immun* **72**, 3733-42.
44. Das, M., Hart-Van Tassell, A., Urvil, P. T., Lea, S., Pettigrew, D., Anderson, K. L., Samet, A., Kur, J., Matthews, S., Nowicki, S., Popov, V., Goluszko, P. & Nowicki, B. J. (2005) *Infect Immun* **73**, 6119-26.
45. Jouve, M., Garcia, M. I., Courcoux, P., Labigne, A., Gounon, P. & Le Bouguenec, C. (1997) *Infect Immun* **65**, 4082-9.
46. Plancon, L., Du Merle, L., Le Friec, S., Gounon, P., Jouve, M., Guignot, J., Servin, A. & Le Bouguenec, C. (2003) *Cell Microbiol* **5**, 681-93.
47. Selvarangan, R., Goluszko, P., Popov, V., Singhal, J., Pham, T., Lublin, D. M., Nowicki, S. & Nowicki, B. (2000) *Infect Immun* **68**, 1391-9.
48. Simons, K. & Toomre, D. (2000) *Nat Rev Mol Cell Biol* **1**, 31-9.
49. McCaw, S. E., Liao, E. H. & Gray-Owen, S. D. (2004) *Infect Immun* **72**, 2742-52.

FOOTNOTES

*This work was supported by grant DK-064229 from the National Institute of Diabetes Digestive and Kidney Diseases and The Wellcome Trust. We are grateful to Evgeni Sokurenko, Veronika Chesnokova and Konstantin Korotkov for helpful criticism of the manuscript, Anh-Linh Bui and Diane Capps for technical assistance. We thank Dr. John E. Shively (Beckman Research Institute City of Hope, Duarte, CA) for generously providing the construct for CEA N-A3 expression. We also thank David J. Evans (Institute of Virology, University of Glasgow) for kindly providing the constructs for DAF expression.

¹The abbreviations used are: DAF: decay accelerating factor. UTI: urinary tract infection. SPR: surface plasmon resonance. MRHA: mannose resistant hemagglutination assay. CEA: carcinoembryonic antigen. CEACAM: CEA - related cell adhesion molecule. CEA N-A3: CEA containing N and A3 domains. N-CEA: CEA containing N domain. NMR: nuclear magnetic resonance. DAEC: diffusely adhering *Escherichia coli*. GPI: glycosylphosphatidylinositol. PBS: phosphate-buffered saline. Cm: chloramphenicol. Amp: ampicillin.

FIGURE LEGENDS

Fig. 1. CEA binding assay with radiolabeled bacteria expressing Dr family adhesins. Bacterial cells were labeled with ³H-thymidine and incubated in microtiter wells coated with soluble CEA at concentrations of 15, 10, 5, or 3 mg/ml. Bound bacteria remaining in the wells were quantified by scintillation counting. Results shown are the average of three independent experiments with duplicate wells of each sample. Error bars indicate standard deviation.

Fig. 2. The N-domain of CEACAMs is important for Dr adhesin binding. A) Sequence alignments for N domains of CEACAMs. B) CEA binding assay with *E. coli* expressing DraE and AfaE-III. Bacterial cells were labeled with ³H-thymidine and incubated with or without the competitor in microtiter wells coated with soluble CEA at a concentration of 5 mg/ml. Competitors were added at final concentrations of 20 μM N-CEA, 80 μM DAF, and 10 mM Cm. Bound bacteria remaining in the wells were quantified by scintillation counting. Results shown are the average of three independent experiments with duplicate wells of each sample. Error bars indicate standard deviation.

Fig. 3. SPR measurement of N-CEA affinity (K_D) to Dr adhesins. A) SPR binding curves of the interaction between N-CEA and DraE fimbriae in steady state. The resulting data were analyzed with BIAevaluation 3.0 software to globally fit data and derive the dissociation constants (K_D). A fit of these data is shown. RU, relative units. RE, response equilibrium. B) Bar chart showing a comparison of dissociation constants (K_D) for different Dr adhesins.

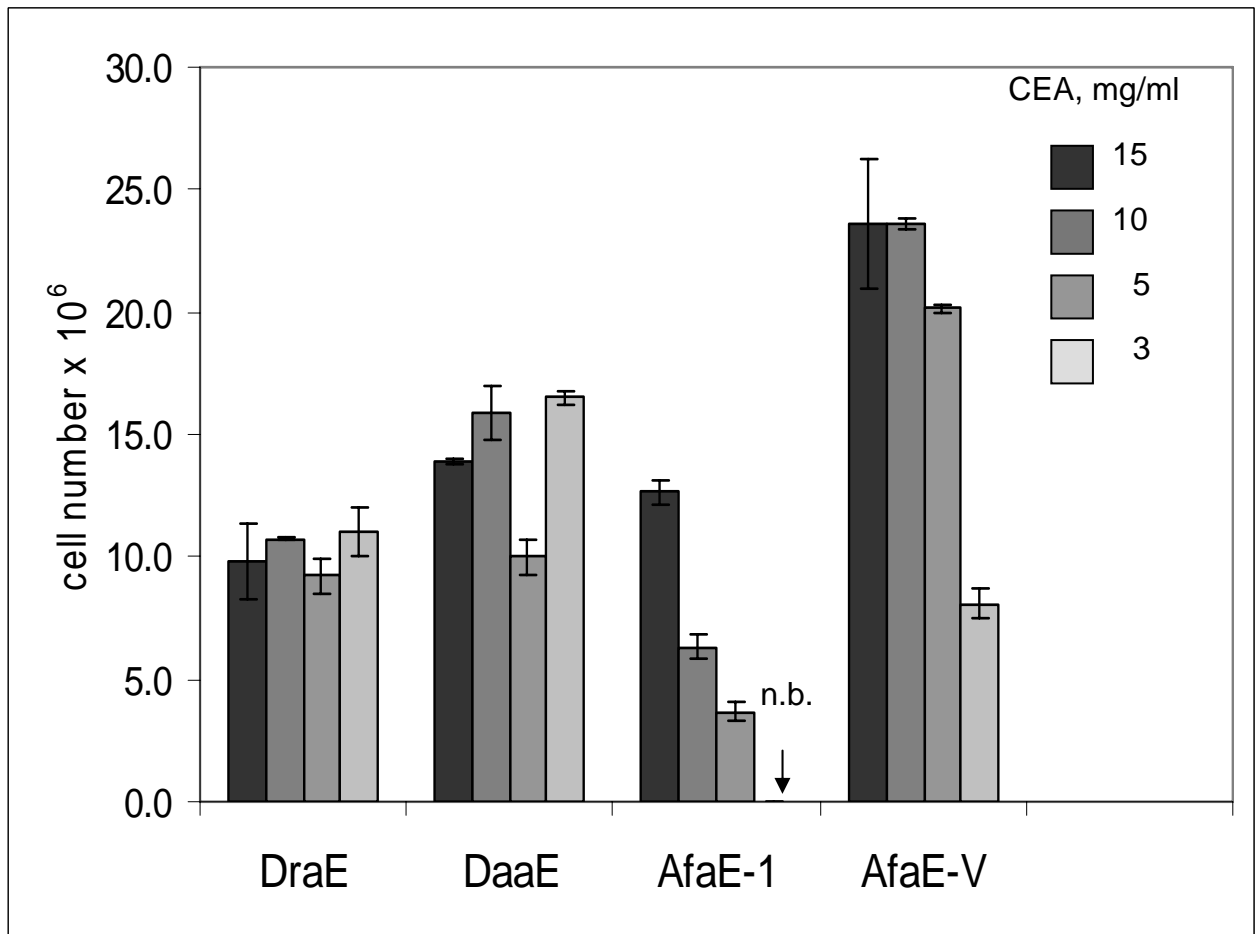
Fig. 4. N-CEA affinity (K_D) for DraE mutants and naturally-occurring DraE/AfaE-III adhesins. A) DraE mutants and B) DraE/AfaE-III-related adhesins determined by SPR. Fimbriae were immobilized on a CM5 sensor chip. N-CEA was dissolved in running buffer and injected over the surface at a flow rate of 20 μl/min for 2 min. Average equilibrium responses were measured for seven concentrations of N-CEA. The resulting data were analyzed with BIAevaluation 3.0. Reported K_D s are the average of at least three independent experiments. Error estimates were propagated from the SE of the K_A .

Fig. 5. Chemical shift mapping of the N-CEA/AfaE-III interaction. A) Region of the 2D ¹H-¹⁵N HSQC spectrum of AfaEIII-*dsc* in the absence (black) and presence (red) of excess N-CEA. Peaks undergoing significant shift changes and/or broadening are labelled. B) Combined surface and ribbon representation of AfaE-III-*dsc* with perturbed amide resonances upon N-CEA addition colored in dark blue, Cm shown in stick representation and position of mutants with altered CEA binding in cyan. C) Surface and ribbon representation of AfaE-III-*dsc* with NMR-derived binding sites for CEA and DAF colored blue and green respectively with Cm as a yellow stick representation (31, 33). Orientation is chosen is approximately 90_y^o rotation relative to Figure 5,B D) Surface and ribbon representation (yellow) of a homology model of human N-CEA derived from the crystal structure of murine N-CEACAM1 (34). Solvent exposed mutant residues that display altered DraE binding are shown in blue.

Fig. 6. DraE/AfaE-III adhesin binding-associated surfaces. Surface representation of AfaE-III-*dsc* with Cm as a yellow stick representation (31, 33). Orientation of A-C the same as D-F, respectively. A-C) DAF (28) and CEA binding sites derived from DraE mutagenesis are shown in green and red, respectively. D-F) DAF-specific interactions derived from chemical shift mapping analysis of AfaE-III-

dsc shown in blue (31). CEA-specific interactions derived from chemical shift analysis of AfaE-III-dsc is shown in dark red. Chemical shift mapping of interactions common to DAF and CEA shown in orange (31).

Figure 1



Note: n.b – no binding

Figure 2

A

CEACAM3 1 KLTIESMPLSVAEGKEVLLLVHNLPOHLFGYSWYKGERVDGNSLIVGYVIGTQQATPGAA
 CEACAM6 1 KLTIESTPFNVAEGKEVLLLAHNLPOHRIIGYSWYKGERVDGNSLIVGYVIGTQQATPGPA
 CEACAM1 1 QLTIESMPFNVAEGKEVLLLVHNLPOQLFGYSWYKGERVDGNROIVGYAIGTQQATPGPA
 CEA 1 KLTIESTPFNVAEGKEVLLLVHNLPOHLFGYSWYKGERVDGNROIVGYVIGTQQATPGPA
 CEACAM8 1 QLTIEAVPSNAAGKEVLLLVHNLPODPRGYNWKGETVDANRRIIGYVINSOQITPGPA

CEACAM3 61 YSGRETIYTNASLLIQNVTDNDIGFYTLQVIKSDLVNEEATGQFHVYQEN
 CEACAM6 61 YSGRETIYPNASLLIQNVTDNDTGFYTLQVIKSDLVNEEATGQFHVYPEL
 CEACAM1 61 NSGRETIYPNASLLIQNVTDNDTGFYTLQVIKSDLVNEEATGQFHVYPEL
 CEA 61 YSGRETIYPNASLLIQNVTDNDTGFYTLQVIKSDLVNEEATGQFHVYPEL
 CEACAM8 61 YSNRETIYPNASLLMRNVTRNDTGSYTLQVIKLNLMSEEVTGQFSVHPET

B

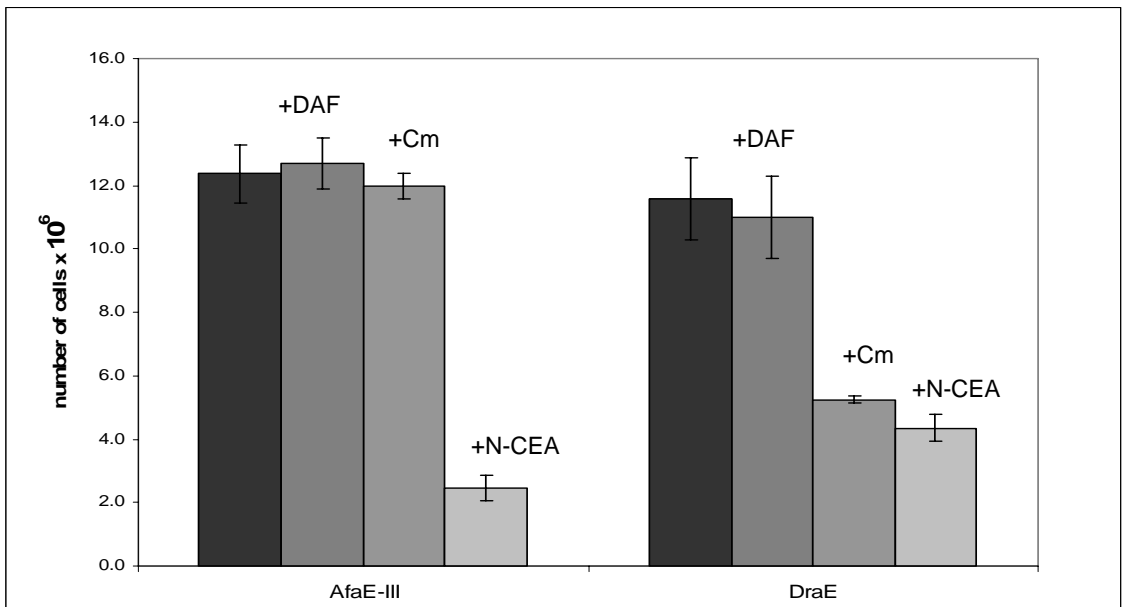


Figure 3

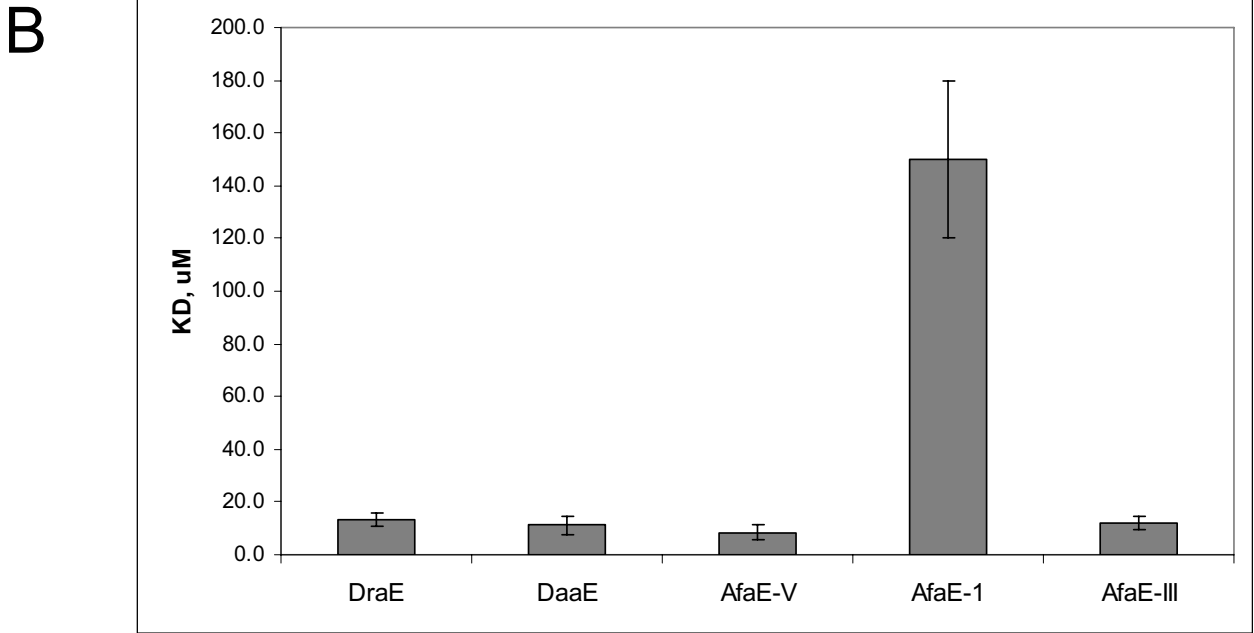
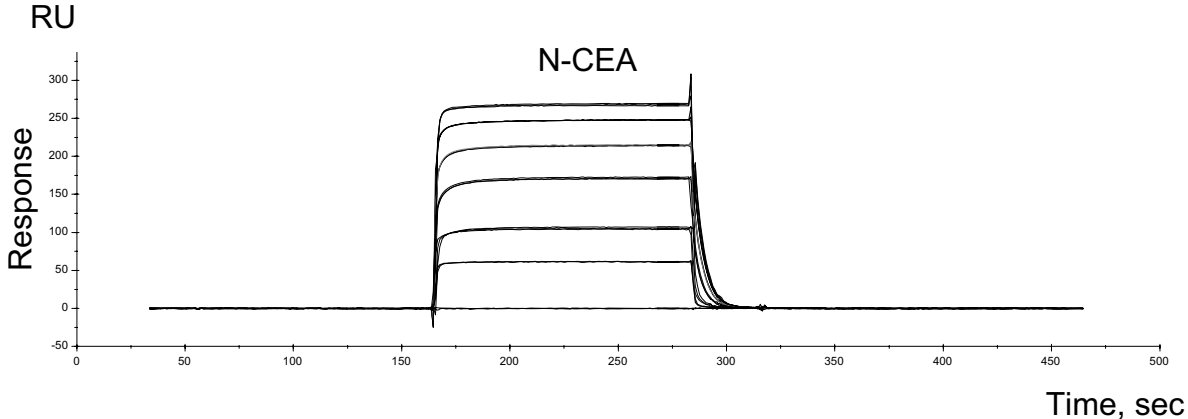
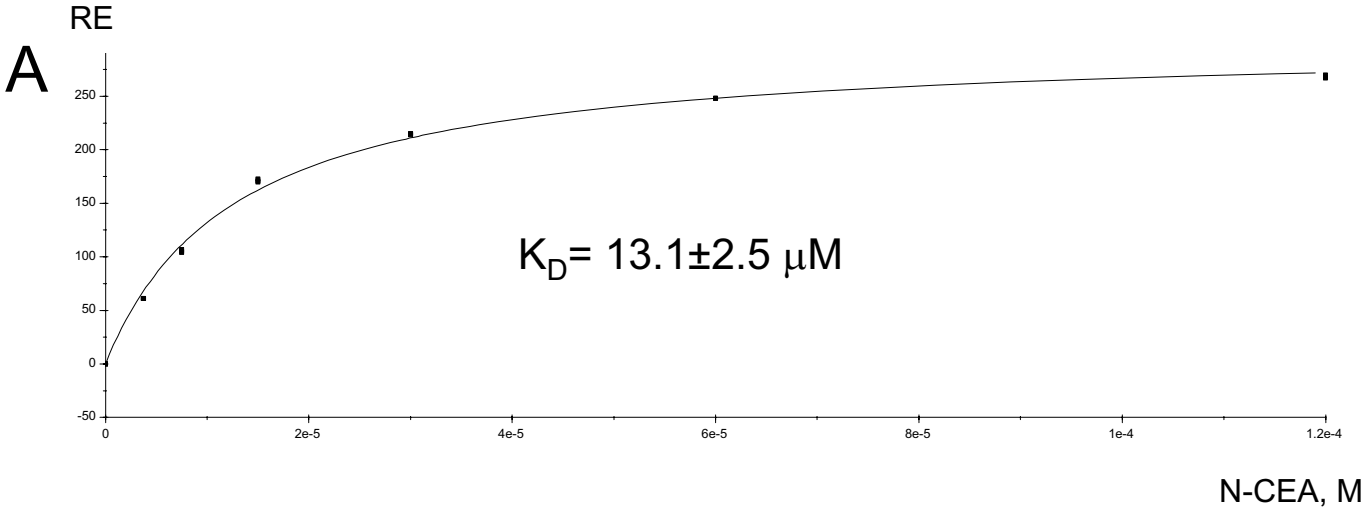
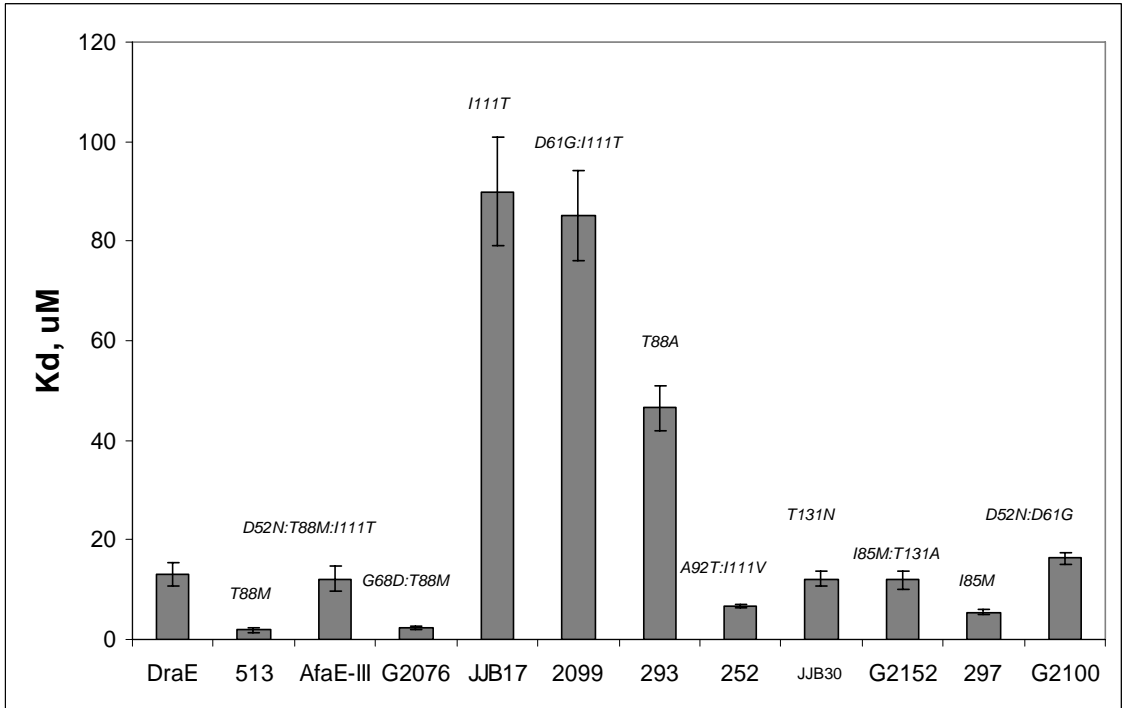


Figure 4

A



B

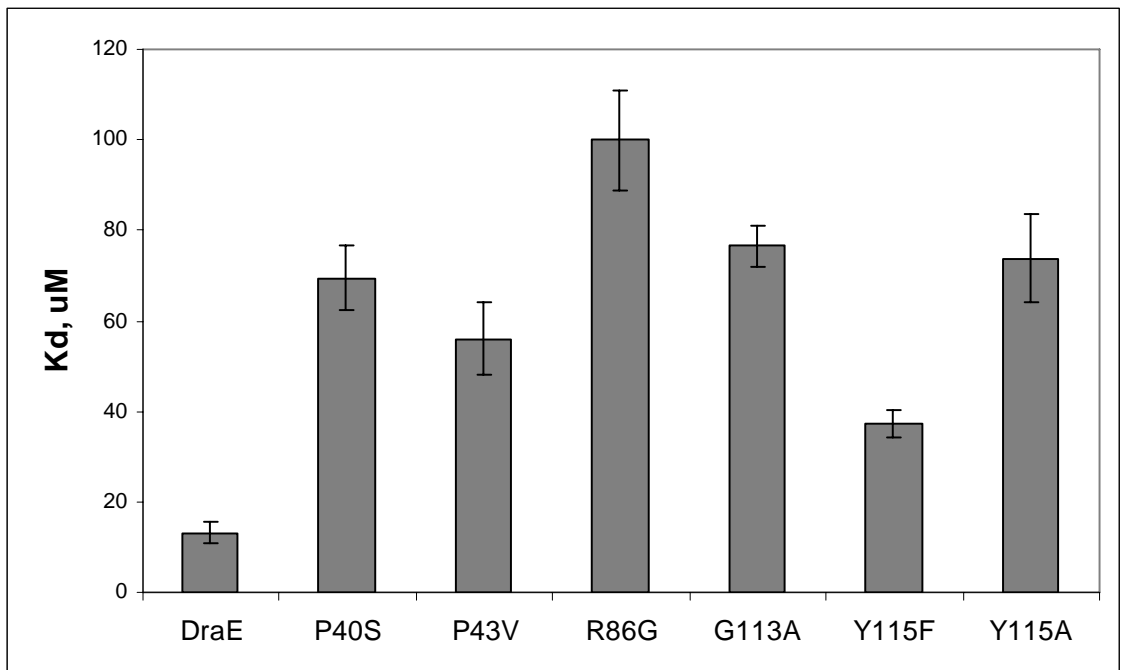


Figure 5

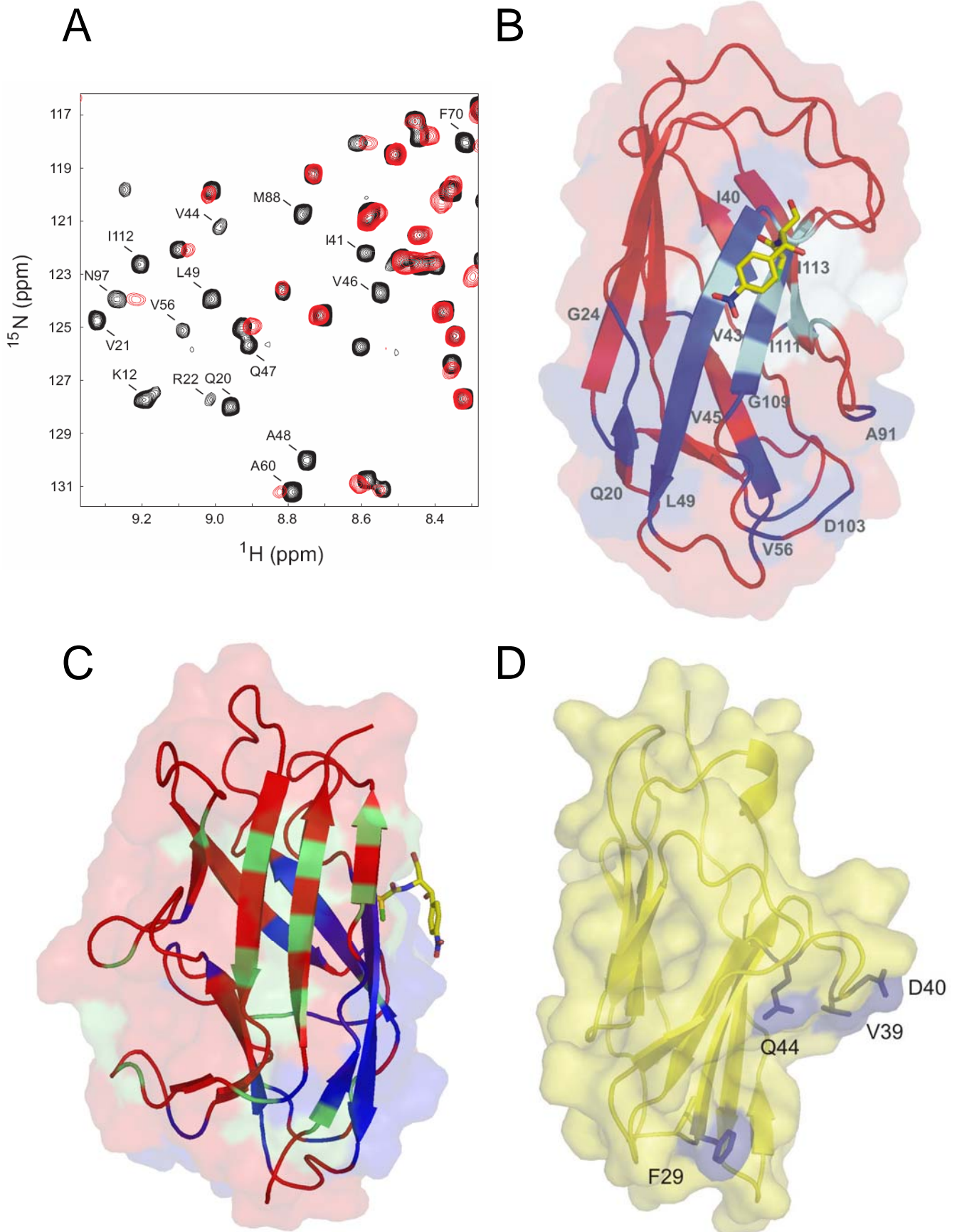


Fig. 6

